Experimental and theoretical analysis of eccentrically loaded brickwork

A. Brencich, C. Corradi and L. Gambarotta
University of Genoa, Department of Civil and Environmental Engineering, Genoa, Italy

ABSTRACT: The compressive strength of masonry plays a central role in the assessment of masonry structures. In spite of a large number of data and theoretical approaches, the failure of brickwork pillars and arches and its dependence on the strength and geometry of the constituents, on the masonry bond and on the loading conditions seems not yet clear. In this paper, concentric and eccentric loading are analyzed both theoretically and experimentally. A mechanical model for eccentrically loaded pillars has been formulated to relate masonry strength to the brick properties. Tests have been performed on brickwork prisms with different load eccentricities. Comparisons between theoretical and experimental results are discussed.

1 INTRODUCTION

Eccentric loading is a primary issue for two classes of technical problems involving masonry structures: *i*) load carrying capacity of walls, vaults, arches and pillars; *ii*) resistance of veneer walls to lateral (wind) pressure. Even though these two problems are quite different, they share a common approach to the definition of material strength. Assuming a pure No-Tensile-Resistant model Perfectly-Brittle in compression, some authors observed an increase of the compressive strength with the load eccentricity (Hatzinikolas 1980, Drysdale 1993, Martinez 2003, Martin Caro 2004) up to 60% more than the value for concentric loading; this means that the compressive strength of masonry would no longer be purely a material parameter. Other authors (Maurenbrecher 1983, Brencich 2005, Cavaleri 2005), instead, considered the compressive strength as a material parameter deduced from tests on the basis of a constitutive model. If the inelastic strains of masonry are taken into account, no increase in compressive strength with load eccentricity is found. Only one code allows a strength increase for eccentric loading (UIC 1995), with an increase up to 60% of the concentric value.

In this paper a procedure for the evaluation of the strength of eccentrically compressed masonry is discussed considering plastically admissible states of an inhomogeneous perfectly-plastic periodic material, varying the geometry and the mechanical characteristics of the brick units. The problem is formulated as an application of the Static Theorem of Limit Analysis. A series of displacement-controlled experimental tests under either concentric and eccentric loading have been carried out on two series of specimens.

2 LIMIT ANALYSIS OF ECCENTRICALLY COMPRESSED PILLARS

A brickwork pillar may be represented by a stack of bricks (width *h,* height *b*) and mortar joints (height *a*), Figure 1.a. Since the bricks are periodically distributed, a unit cell representative of the whole brickwork can be recognized, Figure 1.b, which is furthermore reduced to that of Figure 1.c because of symmetry conditions. B^b represents the bricks and B^a the mortar domains.

Since the stack has a relevant depth, plain strain conditions are considered and the analysis is carried out by referring to a thickness (in the third direction) equal to one.
In order to evaluate the limit axial force for a given eccentricity $e = M/N$ (N : axial thrust, $M=Ne$: bending moment, N: axial thrust), the Static Theorem of Limit Analysis can be applied obtaining equilibrated stress fields in terms of two Airy stress functions for the mortar, Φ^a, and for the brick, Φ^b, domains. Static boundary conditions on the bases ∂B_d and ∂B_u, Figure 1, are expressed as:

$$\int_{\partial B_d} \Phi^a_{,xx} dx = \int_{\partial B_u} \Phi^b_{,xx} dx = N , \qquad \int_{\partial B_d} \Phi^a_{,xx} x\, dx = \int_{\partial B_u} \Phi^b_{,xx} x\, dx = N \cdot e = M , \tag{1}$$

where the subscripts represent the second derivatives with respect to the x variable. Due to symmetry conditions on the bases ∂B_d and ∂B_u with respect to horizontal planes, cutting at mid-height both the brick unit and the mortar layer gives:

$$\Phi^\alpha_{,xy} = \Phi^\alpha_{,yyy} = \Phi^\alpha_{,xxy} = 0, \qquad \alpha = a, b, \tag{2}$$

while the condition of free lateral edges, ∂B_r and ∂B_l, Figure 1, is expressed in the form:

$$\Phi^\alpha_{,yy} = \Phi^\alpha_{,xy} = 0, \qquad \alpha = a, b. \tag{3}$$

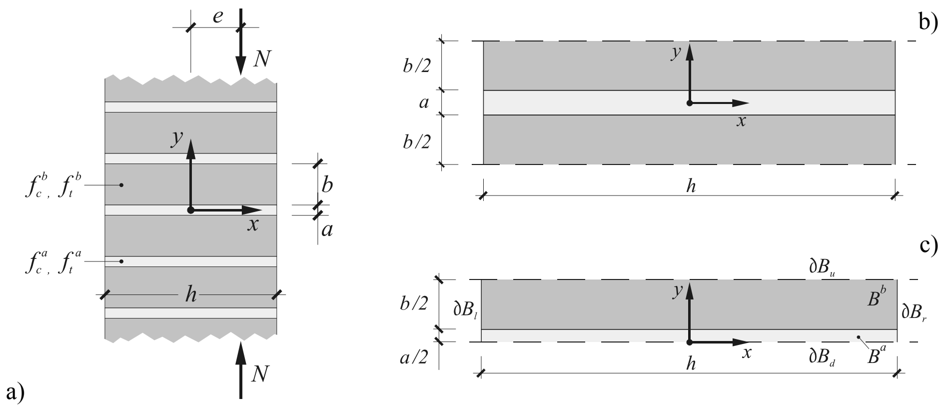

Figure 1. a) Eccentrically compr. column; b) unit cell; c) representative volume element.

In order to simplify the analysis, a subset of the equilibrated stress fields is considered:

$$\Phi^\alpha(x,y) = a_0 f_0(x) + \sum_{n=1}^{N}\sum_{m=1}^{M} a^\alpha_{nm} f^\alpha_n(x) g^\alpha_m(y), \tag{4}$$

where the functions $f_n^\alpha(x)$ ($n = 0,\dots, N$), $g_m^\alpha(y)$ ($m = 1,\dots, M$) are polynomials properly selected in order to satisfy boundary conditions given in eq. (2) and the parameters a_0 and a^α_{nm} ($\alpha = a, b$; $n = 1,\dots, N$; $m = 1,\dots, M$) are unknowns. By collecting these variables in vector $\mathbf{a}$, the stress function representative of the stress fields in the brick B^b and in the mortar B^a domains can be expressed in the form $\Phi^\alpha = \boldsymbol{\Phi}^{\alpha\,T}\,\mathbf{a}$ ($\alpha = a, b$),$\boldsymbol{\Phi}^\alpha$ being a vector collecting elementary stress functions according to eq. (4).
The Mohr-Coulomb limit domain is assumed for brick units and mortar. In order to obtain a linear programming formulation of the problem, the Mohr-Coulomb domain is piecewise linearized with K planes in the space of the stress components (Sloan 1988) and expressed by the linear inequalities:

$$(\mathbf{m}^\alpha_k)^T\,\mathbf{L}(\boldsymbol{\Phi}^\alpha)^T\,\mathbf{a} \le D^\alpha, \quad k = 1,\dots, K \quad \text{in } B^\alpha, \quad \alpha = a, b. \tag{5}$$

The plastic admissibility of the stress field is imposed on a limited number of points ($P\times Q$) in the bricks and mortar:

$$\mathbf{M}^\alpha\,\mathbf{L}(\,\boldsymbol{\Phi}^\alpha(x_p, y_q)\,)^T\,\mathbf{a} \le \mathbf{d}^\alpha; \qquad p = 1,\dots, P; \quad q = 1,\dots, Q. \tag{6}$$

Table 1. Main characteristics of the brickwork stack

	Width h [mm]	Height [mm]	Compr. Str. f_c [N/mm^2]	Tens. Str. f_t [N/mm^2]
Brick	250	$b = 55$	1.00	0.100
Mortar	250	$a = 10$	0.25	0.025

At the brick-mortar interface, normal and shear stress continuity is imposed providing a linear homogeneous equation $\mathbf{A}_{Cont}\,\mathbf{a} = \mathbf{0}$, while the Coulomb frictional, No Tensile Resistance law is imposed as an inequality in the form $\mathbf{A}_{Fr\text{-}NTR}\,\mathbf{a} \leq \mathbf{0}$. The load carrying capacity N_c is obtained by solving the linear program:

$$\begin{cases} \max\ N = \mathbf{c}^T\mathbf{a} = a_0 \int_{-h/2}^{h/2} f_0''\,dx \\ \mathbf{S}\ \mathbf{a} \leq \mathbf{d} \\ \mathbf{A}_{Cont}\ \mathbf{a} = \mathbf{0} \\ \mathbf{A}_{Fr\text{-}NTR}\ \mathbf{a} \leq \mathbf{0} \end{cases} \quad (7)$$

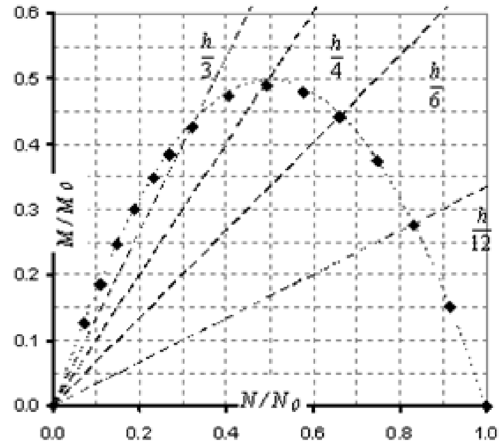

Figure 2. Limit strength domain

The procedure has been applied to the brick stack characterized by the parameters of Table 1; for different values of eccentricity, the ultimate load and the related limit stress state have been evaluated. The results are summarized in the non-dimensional diagram (N/N_0, M/M_0), Figure 2, showing that the limit points are very close to the parabola provided by a simplified model of Euler-Bernoulli homogeneous NTR Elastic-Perfectly-Plastic beam section. This outcome is obtained for varying the value of the ratio $b/ah \in [0.2, 2]$, that shows a limited influence of the edge effects and material parameters mismatch on the stress field.

3 TESTING PROCEDURES

Two types of specimens have been tested to represent two different brickwork bonds: i) type 1: a 110x250x270mm prism of four bricks and five mortar joints; ii) type 2: a 250x250x345mm prism consisting of five levels and six mortar joints with the central level as a symmetry plane, Figure 3. The materials have been characterized by means of a large number of tests according to (prEN 1052-1 1998, prEN 772-1 1999), Table 2, shows the dispersion of experimental data typical of brickwork, is 15-20% of the average value. Mortar 1 is a cement-lime mortar and mortar 2 is a "white cement"-lime-mortar, for which the producer did not give the exact proportions, represent medium and medium-high strength mortars. Brickwork 1 and Brickwork 2 originate from the corresponding mortars.

Loads were applied with eccentricity of 0, 40, 60 and 80 mm (e/h=0, 4/25, 6/25, 8/25, h being the width of the brick), Figure 4, repeating each test at least twice. Displacements were measured in the positions showed in Figure 4; data taken from corresponding points on opposite sides of the specimen allowed the control of undesired lateral eccentricity.

Testing setup is presented in Figure 5; minor details can be found in (Brencich 2004, Corradi 2006). The load measuring device is a C5 class *HBM-RTN* load cell with a 0.01% precision, Figure 5, in-between the upper plate and the testing machine. The loading plates were connected to the testing frame with cylindrical hinges allowing the load line to be precisely identified. The displacements were measured by means of LVDTs with a 1/1200 mm precision; displacements of the upper plate are measured directly under the load line and the lateral ones were recorded close to the ends of the specimen to derive the plates rotation.

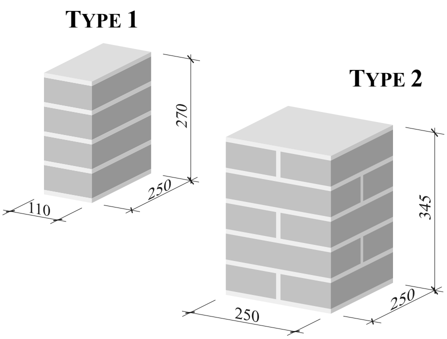

Figure 3. Tested specimens
(Dimensions in mm)

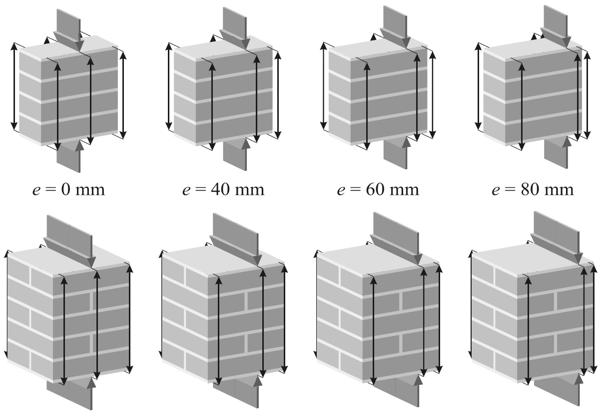

Figure 4. Testing program
(arrows indicate the direction of the applied load)

Table 2. Mechanical characteristics of bricks and mortars.

		Av. Value [N/mm²]	n. of samples	C.o.V.	Char. Value[1] [N/mm²]	Char. / Av.
Brick	Compr. Str.– direct	19.7	20	17%	14.1	0.72
	El. Mod (in compression)	1530	20	30%	765	0.50
	Tens. Str.– TPB	4.7	10	10%	3.9	0.83
	El. Mod (in tension)	920	10	25%	535	0.58
Mortar 1	Compr. Str.– direct	13.1	20	18%	9.2	0.70
	El. Mod (in compression)	1545	20	16%	1130	0.73
	Tens. Str.– TPB	3.4	10	15%	2.6	0.75
	El. Mod (in tension)	1120	10	19%	765	0.68
Mortar 2	Compr. Str.– direct	10.0	20	16%	7.3	0.73
	El. Mod (in compression)	1365	20	22%	865	0.63
	Tens. Str.– TPB	2.7	10	12%	2.2	0.80
	El. Mod (in tension)	1365	10	23%	535	0.62

[1]: Assuming a Gaussian distribution

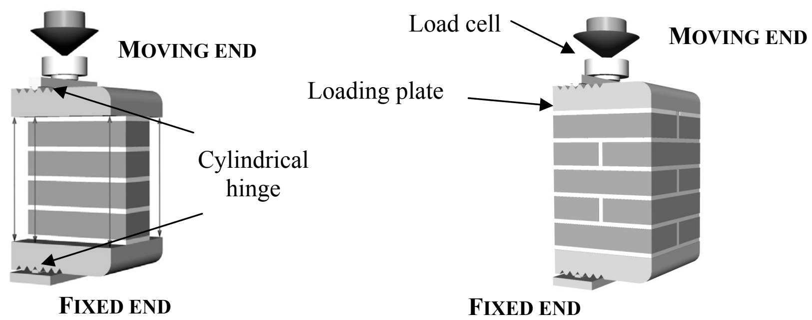

Figure 5. Test setup

The tests for type 1 specimens have been displacement controlled, being the lower hinge (connected to the testing frame) and the one over the load cell moved by a mechanical device; the load is measured by the load cell. A 2 mm thick lead sheet was used between the specimen and the loading plates to smooth the bases of the specimens; friction between the bases and the loading plates could not be removed because eccentric loading without friction would result in highly unstable tests. For type 2 specimens, due to the higher loads, the tests have been force-controlled.

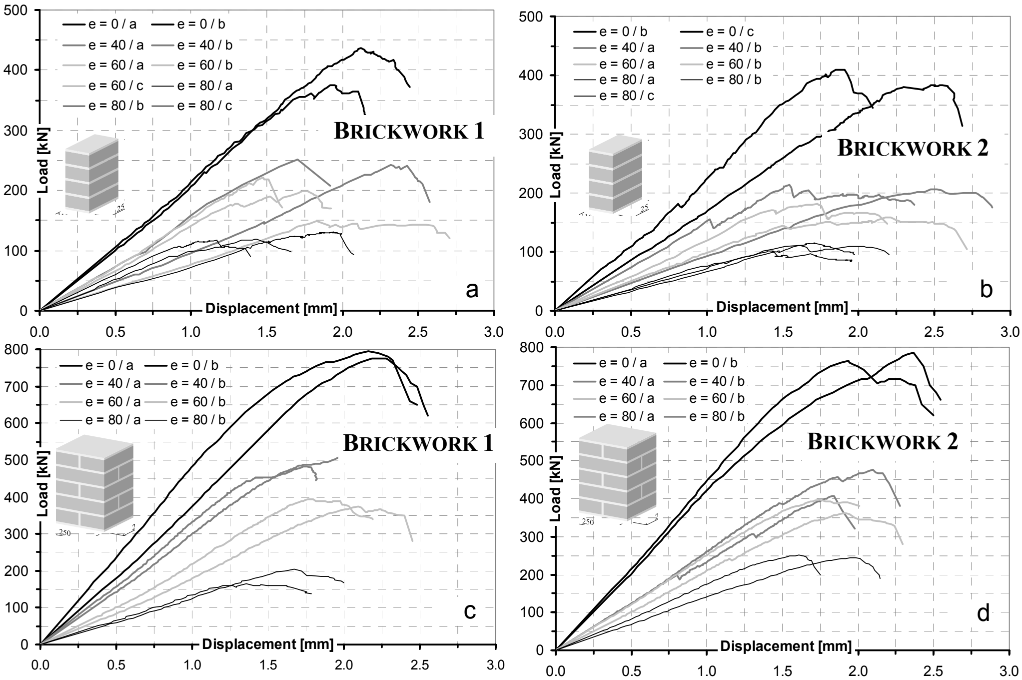

Figure 6. Test results: a) and b) type 1; c) and d) type 2

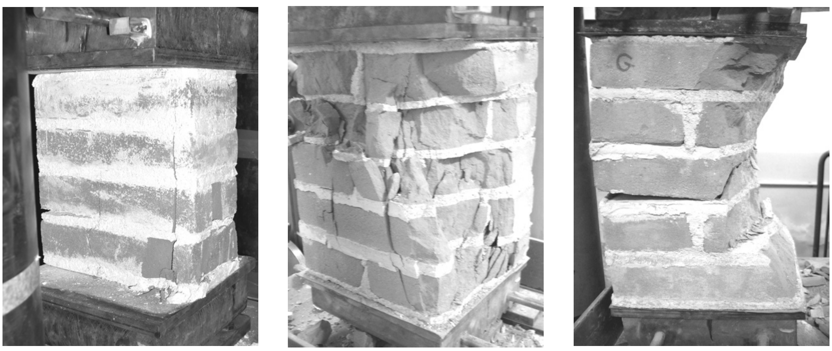

Br. 1 – type 1 – e=60 mm Br. 1 – type 2 – e=0 mm Br. 1 – type 2 – e=60 mm

Figure 7. Collapse mechanism for brickwork 1 under concentric and eccentric loading

Figures 6 shows the load-displacement (just below the load) response of the specimens; concentric, identified as *e*=0, and eccentric load tests clearly show an initial linear behavior followed by an inelastic phase. If the available ductility δ_{av} is defined as the ratio between the ultimate strain ε_u and the value at the end of the elastic limit ε_{el} (Brencich 2005), $\delta_{av}=\varepsilon_u/\varepsilon_{el}$, ductility can be calculated for all the specimens directly from the concentric load tests, Table 3. Figure 7 show the crack patterns at the end of the tests for some specimens.

Looking at the assessment of eccentrically loaded structures, the experimental data are best represented in a $N/N_0 - M/M_0$ plane, being the normalizing quantities N_0 and M_0 the ultimate load for concentric loading and $M_0=N_0 \cdot h/4$ respectively, Figure 8. The model discussed in the previous section, based on Limit Analysis and on the assumption that clay and mortar may be represented by Elastic-Perfectly-Plastic models, led to a limit domain, Figure 2, which is almost identical to what would be obtained for the simple model of a homogeneous NTR Elastic-Perfectly-Plastic section, a parabola in the $N/N_0 - M/M_0$ plane (Drysdale 1993).

Table 3. Experimental data – concentric loading

	Specimen	f_c [N/mm^2]	ε_{el} [%]	ε_u [%]	$\delta_{av}=\varepsilon_u/\varepsilon_{el}$	E [N/mm^2]
BRICKWORK 1	Type 1 - a	12.5	0.64	0.71	1.27	1990
	Type 1 - b	14.5	0.60	0.79	1.51	2080
	Type 1 – av.	**13.5**	**0.62**	**0.75**	**1.39**	**2035**
	Type 2 – a	12.4	0.47	0.65	1.42	2210
	Type 2 – b	12.7	0.56	0.64	1.34	2550
	Type 2 – av.	**12.5**	**0.51**	**0.64**	**1.38**	**2380**
BRICKWORK 2	Type 1 – a	12.8	0.82	0.95	1.16	1610
	Type 1 – b	13.7	0.56	0.70	1.16	2200
	Type 1 – av.	**12.9**	**0.69**	**0.83**	**1.16**	**2085**
	Type 2 – a	12.6	0.55	0.71	1.31	2120
	Type 2 – b	12.2	0.49	0.58	1.44	2500
	Type 2 – av.	**12.4**	**0.52**	**0.64**	**1.37**	**2310**

Figure 8, comparing this parabola (the outer one) to the experimental points, shows that the test data are all inside the Limit Analysis domain. This outcome: i) is not completely unexpected since masonry and its constituents are not ductile materials but rather brittle ones; ii) shows that the Limit Analysis approach of par. 2 overestimates the actual load carrying capacity of the material, which is likely to be ascribed to the inelastic phenomena taking place in clay and mortar and / or at their interface close to the peak load.

4 HOMOGENEOUS MODELS AND COMPRESSIVE STRENGTH

The technical approach to the assessment of an eccentrically loaded brickwork section refers to simple homogenized models in which brickwork is given a one-dimensional constitutive law, the most common of which are: i) a No-Tensile-Resistant Perf.-Brittle constitutive model (NTR-PB), Figure 9.a; ii) a NTR El.-Perf.-Pl. (NTR-EPP) model, Figure 9.b. Both these models need one mechanical parameter: material compressive strength f_c, that may be defined by experimental tests or theoretical approaches. The ductile NTR-EPP model does not fit the actual response of brickwork while the diagrams of Figures 6 show that also the first model, NTR-PB, is unable of representing the inelastic strains showed by the tests. Concentric tests, Figure 6, show that an NTR-EPP model might be assumed provided that the inelastic strains are limited according to the ductility measured in concentric tests, Table 3 and Figure 9.c (NTR-EPP-LAD=No Tensile Resistant – Elastic Perfectly Plastic – Limited Available Ductility).

Concentric loads produce a uniform stress distribution in the section, thus leading to a statically determinate problem; eccentric loads induce a stress distribution that is unknown, leading to a statically indeterminate problem. For these reasons, the definition of compressive strength f_c from concentric tests is straightforward ($f_c=N_c/A$); eccentric load tests lead to different results if different constitutive models are assumed for the material. For a NTR-PB model, the compressive strength $f_c^{NTR\text{-}PB}$ seems to depend on the load eccentricity because of the assumed constitutive law (Hatzinikolas 1980, Drysdale 1993, Martinez 2003, Martin Caro 2004). Other models, such as the NTR-EPP-LAD model, Figure 9.c, show a compressive strength $f_c^{NTR-EPP-LAD}$ independent on the load eccentricity.

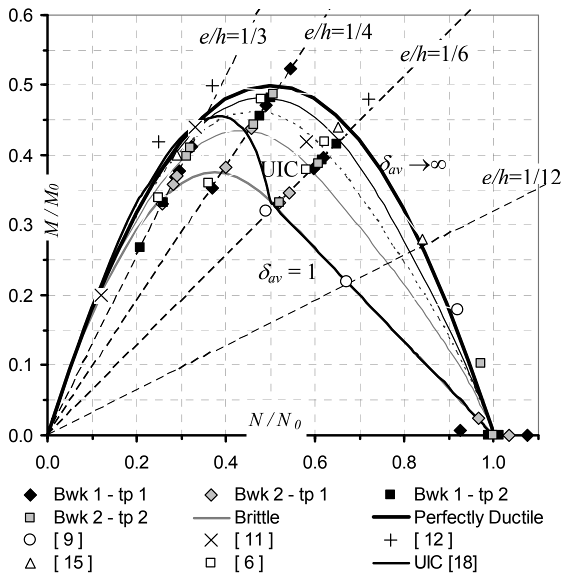

Figure 8. Limit domain of the NTR–EPP model and experimental data in the N/N_0–M/M_0 plane

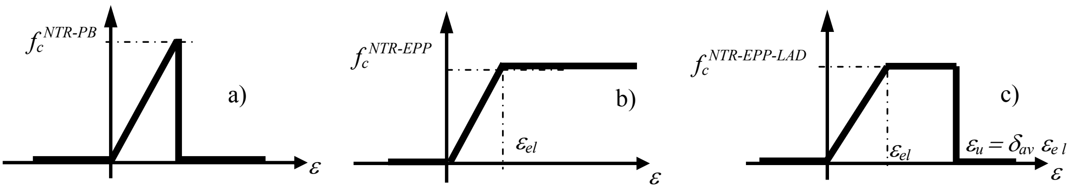

Figure 9. Stress-Strain relationships; a) NTR-PB, b) NTR-EPP; c) NTR-EPP-LAD models

Figure 8 shows the limit domains in the N/N_0–M/M_0 plane for: *i)* the NTR-PB model, Figure 9.a, inner curve (δ_{av}=1); *ii)* the NTR-EPP model, Figure 9.b, and Limit Analysis approach of paragraph 2, outer parabola ($\delta_{av}\rightarrow\infty$); *iii)* the NTR-EPP-LAD model for some values of δ_{av} (δ_{av} =1.25, δ_{av} =1.5, δ_{av} =2, inner lines); *iv)* the experimental data of this research and of some references; *v)* the limit domain curve obtained with the strength increase allowed by UIC (UIC 1995) for high eccentricities.

The experimental points all lie essentially inside two borders: the upper Perfectly-Plastic parabola and the inner NTR curve. Some points lie slightly outside these limits but this is due to the variability of the concentric compressive strength, which is the normalizing quantity. Several points show very limited ductility, while the majority of the experimental tests would be interpreted by an NTR-EPP-LAD model assuming the available ductility δ_{av} in the range [1.2,1.5], as deduced from the concentric tests of Table 3. The widened domain allowed by UIC (UIC 1995) includes in the assumed elastic safe region several experimental points for high eccentricity. Since the collapse of an arch takes place when the axial thrust is highly eccentric (plastic hinge), the widened UIC domain appears to overestimate the load carrying capacity of arches and is therefore unsafe for design. It is worthwhile noting that Euro Code 6 (ENV 1996-1 1998) does not allow any strength increase at all.

5 CONCLUSIONS

The theoretical model discussed in the paper shows that the local perturbations of the stress field, due to both free surface effects and strength mismatch at the mortar joints, play a minor role in the brickwork collapse. With the aim of evaluating the limit domain for a masonry section in the (*N, M*) plane, this result corroborates the assumption of a homogeneous NTR-PP in compression constitutive model for brickwork.
The experimental data provide useful information on the failure mechanism and strength of brickwork for eccentric loading; the comparison with inhomogeneous models and with the simplified NTR homogeneous beam approaches shows that the NTR-Perfectly Brittle model is overconservative. On the contrary, an Elastic-Perfectly-Plastic model better reproduces the tesst outcomes provided that a limit is given to the inelastic strains. Even though the experimental data base needs to be widened, the apparent strength increase due to load eccentricity is related to the internal redundancy of the eccentrically loaded section. Therefore, the strength increase with load eccentricity is only apparent; similar conclusions have been derived on solid clay brickwork (Maurenbrecher 1983, Brencich 2005) and on tuff stone (Cavaleri 2005).
Since the strength increase with load eccentricity is only apparent and due to inelastic phenomena, any assessment procedure in masonry design codes should not consider a strength increase for eccentric loads and not allow any inelastic strain to be developed.

ACKNOWLEDGEMENTS

The authors acknowledge the partial financial contribution by the Italian Network of Seismic Laboratories (RELUIS) - 2005-2008 Pr. "*Safety Assessment and vulnerability reduction of existing bridges*" – Line 3 and by the Italian Dept. of Univ. and Sc. Res. (MIUR) for the 2003 COFIN Project "*Safety, maintenance and management of masonry bridges.*"

REFERENCES

Brencich 2004: Brencich, A., Corradi, C., Sterpi, E. "Experimental approaches to the compressive response of solid clay brickwork", Proc. 13th IBMaC., 4-7 July, Amsterdam.

Brencich 2005: Brencich, A., Gambarotta, L. "Mechanical response of solid clay brickwork under eccentric loading. Part I: Unreinforced Masonry", Mat. and Str., **38**, 257-266.

Cavaleri 2005: Cavaleri, L., Failla, A., La Mendola, L., Papia, M. "Exp. and analyt. response of masonry elements under eccentric vertical loads", *Eng.ng Str.s,* **27**, 1175-1184.

Corradi 2006: Corradi, C. "Theoretical and experimental analysis of the strength of eccentrically loaded brickwork" (in Italian), Ph.D. Thesis, Univ. of Genoa.

Drysdale 1993: Drysdale, R.G., Hamid, A.A., Baker, L.R. "Masonry Structures, Behaviour and Design", Prentice Hall, Englewood Cliffs.

ENV 1996-1-1 1998: EURO CODE 6. "Design of masonry structures, Part 1-1: General rules for buildings – Rules for reinforced and un-reinforced masonry".

Hatzinikolas 1980: Hatzinikolas, M., Longworth, J., Warwaruk, J. "Failure modes for eccentrically loaded concrete block masonry walls", ACI J.nl, 77, 258-263.

Martinez 2003: Martinez, J.L.M. "Theoretical and experimental determination of the limit domains of masonry structures, and application to historical structures", Ph.D. Thesis, T. U. of Madrid.

Martin Caro 2004: Martin Caro, J.A., "Masonry compressive strength enhancement under eccentric axial load", Proc. 4th Arch Bridge Conf., Barcellona, 2004, Roca and Molins ed.s, CIMNE, Barcellona, 2004, 405-412.

Maurenbrecher 1983: Maurenbrecher, A.H.P. "Compressive strength of eccentrically loaded masonry prisms", Proc. of the 3rd Can. Mas. Symp., Edmonton, 10/1-10/13.

UIC 1995: UIC – International Union of Railways: UIC code 778-3R, "Recommendations for the assessment of the load carrying capacity of the existing masonry and mass-concrete arch bridges".

prEN 772-1.1999. "Methods of test for masonry units-Part1: Determination of compr. strength"

prEN 1052-1.1998. "Methods of test for masonry-Part1: Determination of compr. strength"

Sloan 1988: Sloan, S.W. "Lower bound limit analysis using finite elements and linear programming", Int. J. Numer. Anal. Methods Geomech, 12, 61-67.